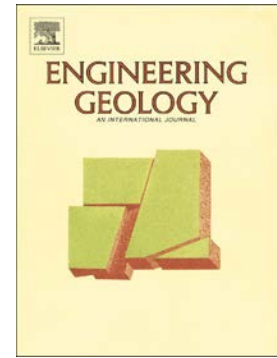


## Accepted Manuscript

From landslide susceptibility to landslide frequency: A territory-wide study in Hong Kong

Florence W.Y. Ko, Frankie L.C. Lo



PII: S0013-7952(17)30925-0  
DOI: [doi:10.1016/j.enggeo.2018.05.001](https://doi.org/10.1016/j.enggeo.2018.05.001)  
Reference: ENGE0 4833  
To appear in: *Engineering Geology*  
Received date: 22 June 2017  
Revised date: 20 February 2018  
Accepted date: 1 May 2018

Please cite this article as: Florence W.Y. Ko, Frankie L.C. Lo , From landslide susceptibility to landslide frequency: A territory-wide study in Hong Kong. The address for the corresponding author was captured as affiliation for all authors. Please check if appropriate. *Enggeo*(2018), doi:[10.1016/j.enggeo.2018.05.001](https://doi.org/10.1016/j.enggeo.2018.05.001)

This is a PDF file of an unedited manuscript that has been accepted for publication. As a service to our customers we are providing this early version of the manuscript. The manuscript will undergo copyediting, typesetting, and review of the resulting proof before it is published in its final form. Please note that during the production process errors may be discovered which could affect the content, and all legal disclaimers that apply to the journal pertain.

**From landslide susceptibility to landslide frequency: a territory-wide study in Hong Kong**

## Author 1

Florence W. Y. Ko BEng LLB MA MSc DIC MHKIE MICE CEng  
Senior Geotechnical Engineer, Geotechnical Engineering Office, Civil Engineering and Development  
Department, Government of the Hong Kong Special Administrative Region (HKSAR), Hong Kong

## Author 2

Frankie L. C. Lo BEng MSc DIC MHKIE MIEAust CPEng  
Geotechnical Engineer, Geotechnical Engineering Office, Civil Engineering and Development Department,  
Government of the Hong Kong Special Administrative Region (HKSAR), Hong Kong

**Contact person:**

Name: Mr Frankie L. C. Lo

Address: Civil Engineering and Development Building, 101 Princess Margaret Road, Kowloon, Hong Kong

Email: frankielclo@cedd.gov.hk

**Abstract**

Rain-induced shallow landslide is the major type of landslide that happens on natural terrain in Hong Kong due to its high seasonal rainfall and deep weathering soil profile. The Geotechnical Engineering Office has been in a leading role to steer the risk management of natural terrain landslides in Hong Kong. Recently, the territory-wide rainfall-based landslide susceptibility model (in terms of landslide density per year) has been developed to predict the number of natural terrain landslides that may occur in an anticipated rainfall event. Subsequently, the storm-based landslide density has been transformed to the annual landslide frequency to compile the territory-wide landslide frequency map by incorporating the mean annual frequency of occurrence of different probable rainfall scenarios. The annual rainfall frequency of a particular rainfall scenario is derived from its return period, determined based on the abundant real-time rainfall data at a five-minute interval from 110 automatic raingauges across Hong Kong at an average density of 10 km<sup>2</sup>/gauge. The transformation is discussed in this paper, together with the evaluation of the performance of the landslide frequency map. In addition, the potential applications of the map in Hong Kong and the pitfalls of the common evaluation methods are highlighted.

**Keywords**

Landslide susceptibility, landslide frequency, rainfall, shallow landslides, Hong Kong

## 1 Introduction

“Natural terrain” is commonly used in Hong Kong to denote hillsides that are not significantly modified by human activities. On average, about 300 natural terrain landslides occur every year in Hong Kong and rain-induced shallow landslide is the major type of landslide due to the high seasonal rainfall and deep weathering soil profile. Heavy rainstorms in Hong Kong generally occur during the wet season from April to September and are associated with either low pressure trough or severe tropical cyclones. As a general reference, the mean annual rainfall at the Hong Kong Observatory (HKO)’s Principal Rain gauge was 2398.5 mm between 1981 and 2010.

Landslides from natural terrain can result in serious consequence to life and property in Hong Kong due to its dense urban development on hillsides. The problem is chronic for the impacts of extreme weather events, slope degradation and ever-increasing population and encroachment of new urban development on steep hillsides. Over the past 35 years, the Geotechnical Engineering Office (GEO) has been in a leading role to steer the risk management of natural terrain landslides in Hong Kong to reduce and contain landslide risk within an as low as reasonably practicable level that meets the needs of the public and facilitates safe and sustainable developments. The slope engineering practice and landslide risk management have evolved in response to experience and through continuous improvement initiatives and technology advances (Wong & Ko 2006).

Landslide hazard assessments aims to estimate the spatial and temporal probability of occurrence of landslides in a study area, together with their mode of propagation, size and intensity (Corominas et al, 2014). Frequency assessment (including the spatial and temporal probability) forms a crucial element in landslide hazard assessment. Landslide susceptibility assessment, which subdivides the terrain into zones with different likelihood that landslide may occur, considers the spatial distribution of landslide. However, as noted by Dai and Lee (2001), the landslide susceptibility obtained is not a probability if the dynamic variables, such as rainfall and ground motions, are not taken into account. The temporal probability is thus left unanswered. The frequency of occurrence of landslides can be evaluated using different approaches, such as formal probability and reliability analysis, logic tree methods, frequency analysis based on past landslide events, or correlation with landslide triggers (or the indirect approaches). Some recent work quantifies landslide hazards in magnitude-frequency relationships considering the frequency of occurrence of each corresponding intensity (e.g. Hungr et al, 1999; Lari et al, 2014), largely based on the approach for probabilistic seismic hazard analysis proposed by Cornell (1968). These tools are fairly well developed, and more discussions are given in IUGS Working Group on Landslide (1997) and Corominas et al (2014).

Recently, Ko & Lo (2016) developed a territory-wide rainfall-based landslide susceptibility model by correlating a comprehensive landslide inventory and selected attributes, including slope angle, lithology, and rainfall. It is capable of predicting the natural terrain landslide density (in the unit of number of landslides/km<sup>2</sup>/year) with the rainfall explicitly considered as a dynamic variable. The rainfall scenarios are classified into 6 classes based on the maximum rolling 24-hour rainfall. The normalisation is based on the mean annual rainfall at the particular location over a period of 30 years (1977-2006). This gives an opportunity for estimating quantitatively the expected annual initiation frequency of landslides on natural hillsides in Hong Kong given that the frequency of occurrence of each rainfall scenario is known. This paper presents the development and validation of a high-resolution territory-wide natural terrain landslide frequency map covering all natural hillsides throughout Hong Kong (with an area of about 660 km<sup>2</sup>) based on the above model. The map considers both the spatial and temporal probabilities of landslide occurrence on natural hillsides in Hong Kong. The mode of propagation, size and intensity of landslides can be assessed separately and mathematically combined with the frequency of occurrence later to assess the landslide hazard (Roberds, 2005).

## 2 History of Hong Kong’s Landscape Evolution

Wong (2009) gave a summary account of the history of Hong Kong’s landscape evolution, which sets the background scene for the on-going mass wasting process and its serious consequence to life and property in the area. In a gist, Hong Kong has a population of over 7 million and a land area of about 1,100 km<sup>2</sup>. The terrain is hilly, with some 75% of the land steeper than 15° and over 30% steeper than 30°. Intense urban development has taken place on flat ground and in foothill areas, and is progressively encroaching on steep hillsides where landslides from man-made slopes and natural terrain may pose a significant hazard (Fig. 1). With the highly populated developments along the foothill areas, even a small failure on natural terrain can cause devastating life and economic consequences.



**Fig. 1.** High concentration of developments in Hong Kong mingled with steep natural hillsides (Ko & Lo, 2016).

According to Wong (2009), natural terrain occupies about 60% of the land and much of it is steeply sloping and mantled by weak saprolitic or residual soils, or colluvial deposits derived from past landslide and erosion processes. While Hong Kong's natural hillsides have experienced a long history of landscape evolution, they remain highly susceptible to rainfall-induced landslides as they are subject to continual degradation. Field investigations have revealed that failures typically occur within one to two meters of the surface mantle, where erosion pipe holes, dilation and partial infilling of relict discontinuities, and localised tension cracks are often observed. Under this on-going geological and geomorphological processes, much of the natural terrain is only marginally stable over large areas and a large number of shallow landslides can be triggered by heavy rain.

Natural terrain landslides in Hong Kong arise typically from rain-induced shallow failures of the surface mantle of the hillside (Wong et al, 2006). The materials that fail at the source areas of the landslides may include top-soil, colluvium and weathered rock. Most of the landslides are of several hundred cubic meters in volume, but some have developed into massive, mobile debris flows with devastating destructive power. Despite that deep-seated failures rarely occur on the natural terrain of Hong Kong, there are some isolated cases involving a massive volume of debris. Some notable cases include the Shum Wan Road landslide in 1995 (GEO, 1996) and Tsing Shan debris lobe movement (Parry & Campbell, 2003), Shek Pik landslide in 2008 (McMackin et al, 2009) and Sai Wan Road landslide in 2016 (GEO, 2017). Their mass wasting process are mostly controlled by geological structures, such as faults and sheeting joints. Falls of individual boulders from natural terrain into developed areas are also reported from time to time.

On top of the above, Au (1998) provided thorough discussions on rain-induced slope instability in Hong Kong and Hencher & Lee (2010) on landslide mechanisms in weathered terrain in Hong Kong. They gave more information on the characteristics of Hong Kong's natural terrain.

### **3 Methodology**

#### **3.1 Rainfall-based Landslide Susceptibility Model**

A territory-wide rainfall-based landslide susceptibility model was developed to predict the number of natural terrain landslides that may occur in an anticipated rainfall event (Ko & Lo 2016). It adopted rainfall, slope angle and simplified lithology as causal factors. Rainfall and landslide data throughout a period of 23 years (years 1985 to 2006, and 2008) were adopted to develop the correlations. The landslide data was based on the Enhanced Natural Terrain Inventory (ENTLI) of Hong Kong compiled by interpretation of aerial photographs. The inventory contains about 100,000 natural terrain landslides. The slope angle map was derived from a 5 m-grid digital elevation model based on the results of multi-return airborne Light Detection and Ranging (LIDAR) survey. The model is one of the few substantial attempts to introduce rainfall intensity as a predictor in a statistical model. With a few exceptions (e.g. Lee et al, 2016), rainfall is rarely considered in landslide susceptibility analyses carried out elsewhere, as usually adequate rainfall data is neither available nor reliable, which renders relating rainfall to landslide occurrence difficult, if not impossible. It is usually considered in the following ways::

- (a) Effect of transient groundwater response as a result of rainfall is simulated by transient

hydrogeological models (e.g. dynamic infinite slope modelling with rainfall trigger (Baum et al, 2002; Casadei et al, 2003; Simoni, et al 2008; Iverson, 2000). Their use in regional susceptibility analyses are often constrained by the impracticality in obtaining necessary data (e.g. soil layers, shear strength parameters of soils, hydrogeological responses) over an extensive area with sufficient reliability and spatial resolution (Godt et al, 2008).

(b) For heuristics and data-driven approaches, while much of the focus of the previous work was on correlating past landslides activity with relevant terrain attributes (e.g. Guzzetti et al, 1999; Evans & King, 1998; Dai & Lee, 2002), the attention given to rainfall as the main causal factor is relatively limited. Arguably the main reason behind is that the practicality of establishing the correlation between rainfall and landslides is often limited by the spatial and temporal resolution of rainfall data.

(c) Some practitioners have attempted to consider rainfall effect by lumping it with other terrain attributes in the landslide susceptibility analyses (e.g. Bui et al, 2016). To this extent, unless rainfall is largely uniform across the area and across time, it is deceptive to claim predictive capability of any landslide susceptibility map thus developed.

The rainfall-based landslide susceptibility model correlates landslide density with normalised maximum rolling 24-hour rainfall. Sixteen attribute groups, comprising eight classes of slope angle (i.e.  $<15^\circ$ ,  $\geq 15^\circ$ - $20^\circ$ ,  $\geq 20^\circ$ - $25^\circ$ ,  $\geq 25^\circ$ - $30^\circ$ ,  $\geq 30^\circ$ - $35^\circ$ ,  $\geq 35^\circ$ - $40^\circ$ ,  $\geq 40^\circ$ - $45^\circ$  and  $\geq 45^\circ$ ) and two classes of simplified bedrock geology (i.e. intrusive and volcanic-cum-sedimentary) were considered. For each attribute group, the year-based and storm-based correlations between normalised maximum rolling 24-hour rainfall and landslide density (in the unit of number of landslides/ $\text{km}^2$ /year) were obtained. Fig. 2 and 3 show the storm-based correlations for intrusive area and that for volcanic-cum-sedimentary areas respectively.

The following sections presents how the storm-based landslide density has been transformed to the annual landslide frequency to compile the territory-wide landslide frequency map by incorporating the mean annual frequency of occurrence of different probable rainfall scenarios. The annual rainfall frequency of a particular rainfall scenario is derived from its return period, determined based on the abundant real-time rainfall data at a five-minute interval from 110 automatic raingauges across Hong Kong at an average density of  $10 \text{ km}^2/\text{gauge}$ . In addition, the performance of the landslide frequency map has been evaluated and the pitfalls of the common evaluation methods are highlighted.

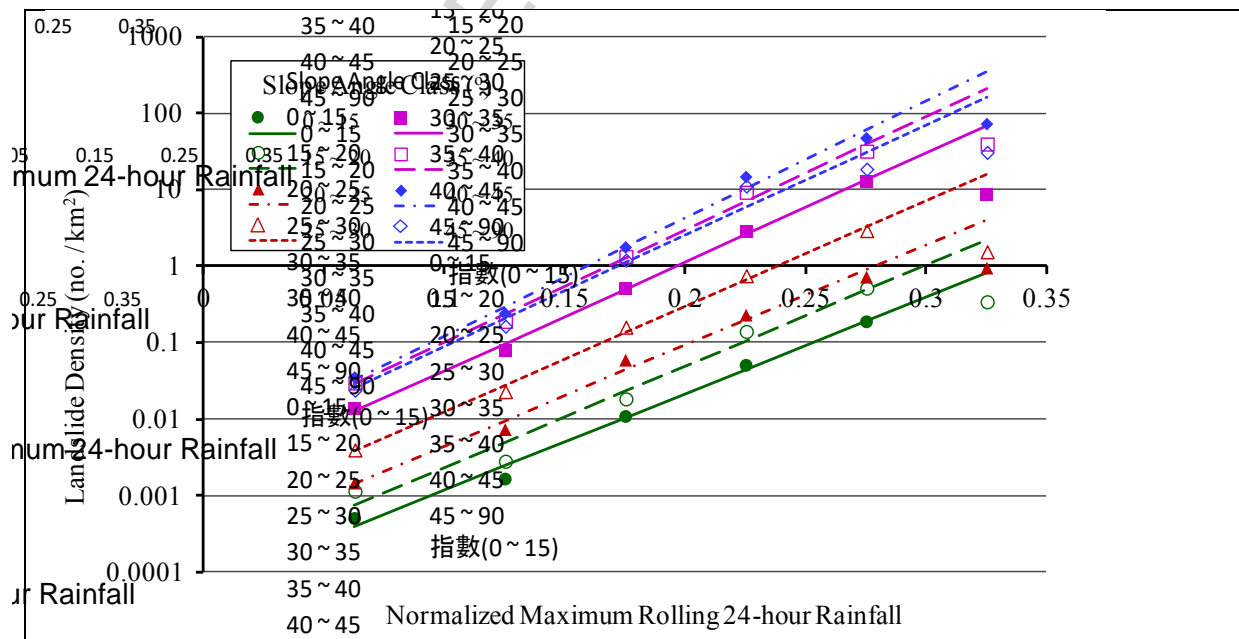


Fig. 2. Storm-based correlation for intrusive area.

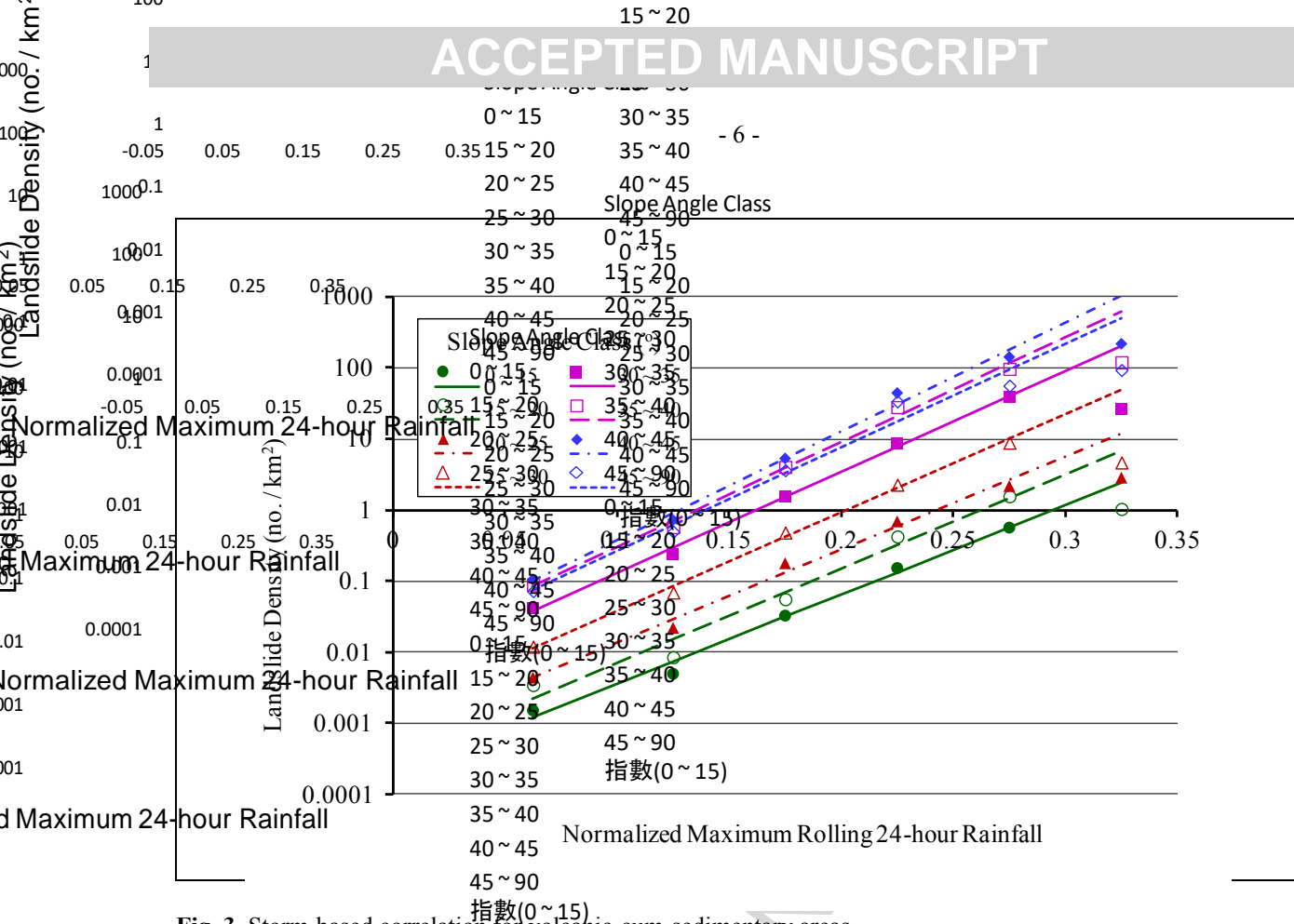
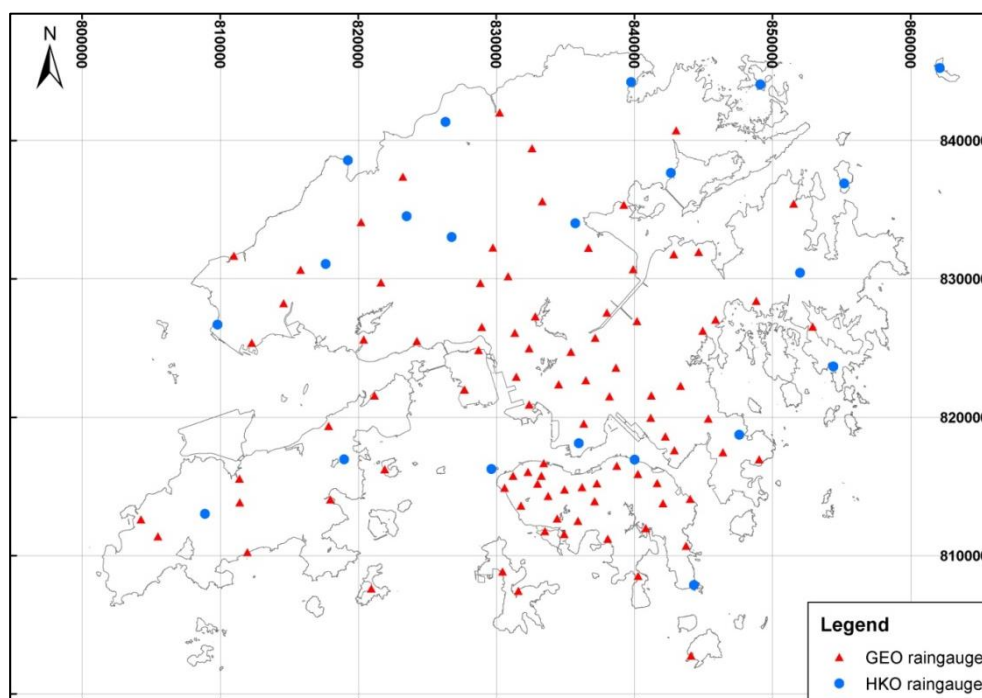


Fig. 3. Storm-based correlation for volcanic-cum-sedimentary areas.

### 3.2 Transformation of Landslide Susceptibility to Landslide Frequency

An annual theoretical landslide frequency (in the unit of number of landslides/year/grid) is the expected number of landslides that would likely occur in a year given the mean annual frequency of occurrence of rainfall, which was calculated as the reciprocal of its return period.

The GEO, together with the Hong Kong Observatory (HKO), has installed 110 automatic raingauges across Hong Kong since the early 1980s. Wong et al (2013) gave a detailed account of the GEO rain gauge system. The existing network comprises 88 GEO and 22 HKO automatic raingauges with an average density of 10 km<sup>2</sup>/gauge (Fig. 4). The raingauges are monitored automatically and real-time rainfall data from the GEO raingauges are transmitted to the GEO Control Centre at a five-minute interval via a mobile data network and Metro Ethernet network services. Data transmission and data sharing between HKO and GEO are carried out by means of dedicated telephone lines. The raingauges provide a reasonably good spatial and temporal coverage of rainfall records across the territory.



**Fig. 4.** Locations of GEO and HKO automatic raingauges.

The more significant rainstorm events (rainstorms with a rolling 24-hour rainfall of over 300 mm anywhere in Hong Kong or those which has resulted in fatal landslides) in the period from 1984 to 2008 are listed in Table 1.

**Table 1.** Significant rainstorm events in the period 1984 to 2008.

| Rainstorm Event No. | Period                | Maximum Rolling Rainfall 24-hr (mm) | Rainstorm Event No. | Period                | Maximum Rolling Rainfall 24-hr (mm) |
|---------------------|-----------------------|-------------------------------------|---------------------|-----------------------|-------------------------------------|
| 1                   | 29/7/1987 - 30/7/1987 | 314                                 | 15                  | 24/8/2000 - 27/8/2000 | 364                                 |
| 2*                  | 20/5/1989 - 21/5/1989 | 552                                 | 16                  | 5/6/2001 - 13/6/2001  | 323                                 |
| 3*                  | 8/5/1992              | 385                                 | 17                  | 6/7/2001 - 7/7/2001   | 301                                 |
| 4*                  | 16/6/1993             | 285                                 | 18                  | 14/9/2002 - 18/9/2002 | 438                                 |
| 5                   | 26/9/1993             | 374                                 | 19                  | 5/5/2003 - 6/5/2003   | 505                                 |
| 6                   | 4/11/1993 - 5/11/1993 | 742                                 | 20                  | 7/6/2003 - 12/6/2003  | 361.5                               |
| 7*                  | 21/7/1994 - 24/7/1994 | 954                                 | 21*                 | 16/8/2005 - 21/8/2005 | 570                                 |
| 8*                  | 5/8/1994 - 6/8/1994   | 380                                 | 22                  | 9/6/2006 - 10/6/2006  | 329.5                               |
| 9*                  | 12/8/1995 - 13/8/1995 | 468                                 | 23                  | 13/9/2006 - 14/9/2006 | 391                                 |
| 10*                 | 2/7/1997 - 3/7/1997   | 799                                 | 24                  | 19/4/2008 - 20/4/2008 | 303                                 |
| 11                  | 8/6/1998 - 9/6/1998   | 562                                 | 25*                 | 6/6/2008 - 9/6/2008   | 622.5                               |
| 12*                 | 22/8/1999 - 26/8/1999 | 565                                 | 26                  | 11/6/2008 - 19/6/2008 | 316.5                               |
| 13                  | 16/9/1999 - 17/9/1999 | 384                                 | 27                  | 25/6/2008 - 1/7/2008  | 378.5                               |
| 14                  | 14/4/2000 - 15/4/2000 | 526                                 |                     |                       |                                     |

Note: This Table includes events with a rolling 24-hour rainfall of over 300mm anywhere in Hong Kong or that which resulted in fatal landslides (annotated with an asterisk after the rainstorm event number).

Since the late 1970s, the GEO has examined the effect of different durations of rainfall on the extent of landslides occurred (Brand et al 1984; Chan et al 2003). Rolling 24-hour rainfall is found to be the most appropriate and convenient parameter for predicting the number of both man-made and natural terrain landslides occurred in Hong Kong (Chan et al 2003; Ko 2005). The combined 4-hour and 24-hour rainfalls may also be

an improved parameter for predicting the number of natural terrain landslides occurred (Wong et al 2004).

By adding up the five-minute rainfall data, year-based (i.e. for a year) normalised maximum rolling 24-hour rainfall across Hong Kong were quantified and related to landslide occurrence, to give a better representation of the severity of the rainfall conditions at any specific location, since the overall rainfall intensity in Hong Kong is unevenly distributed. Year-based normalised maximum rolling 24-hour rainfall at a location is equal to the maximum rolling 24-hour rainfall in a year (in the unit of mm) at the location divided by the mean annual rainfall (1977 to 2006) (in the unit of mm) at the same location (Chan et al 2012). Geostatistical analyses were carried out with the method of Kriging using the available GEO automatic raingauge data to construct rainfall isohyets and derive maximum rolling 24-hour rainfall data. The distribution of mean annual rainfalls across Hong Kong is shown in Fig. 5. Fig. 6 shows the contours of the year-based normalised maximum rolling 24-hour rainfall over the natural terrain area in 2008 as an example.

The sets of curve on return period against normalised maximum rolling 24-hour rainfall, calculated for different raingauge locations using rainfall data between year 1985 and 2000 are shown in Fig. 7. A representative curve for natural terrain was chosen. From this curve, the return periods of the normalised maximum rolling 24-hour rainfall at the boundaries of rainfall scenarios A, B, C and D, i.e. 0.10, 0.20, 0.30 and 0.35 respectively, were identified. By the application of the Poisson statistical model, the annual probability of occurrence and the corresponding return period were calculated for each rainfall scenario (Fig. 8 and Table 2). The mean annual frequency of occurrence of each rainfall scenario is the reciprocal of its return period (Table 2). The values of the mean annual frequency of occurrence of the four rainfall scenarios were first adopted in Wong et al (2006) as one of the components considered in calculating the hazard frequency in the global landslide risk assessment for natural terrain in Hong Kong.

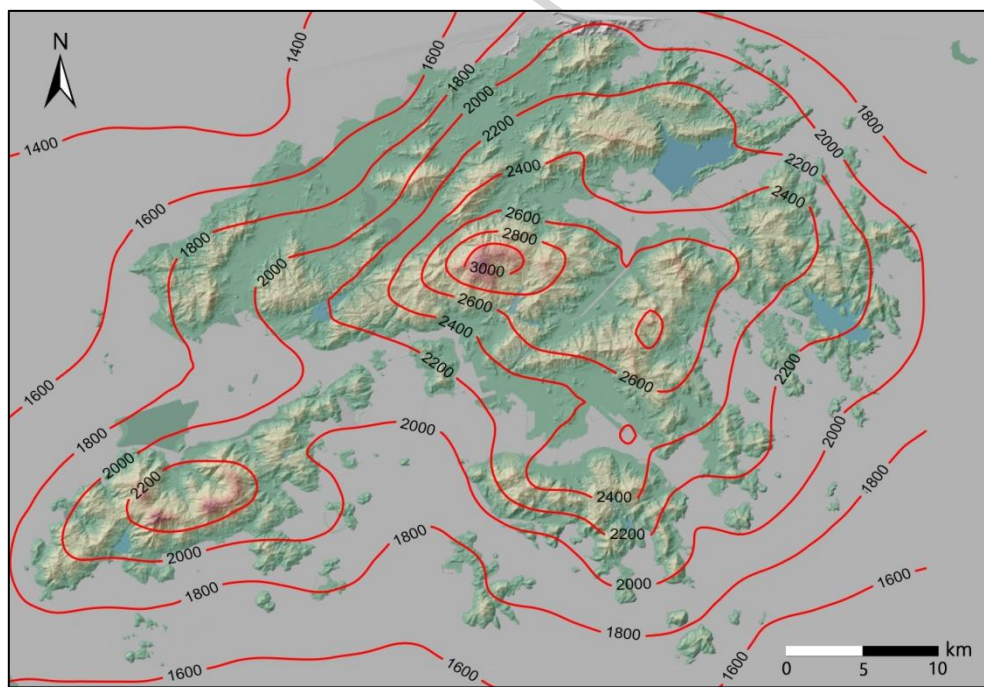


**Fig. 5.** Mean annual rainfall isohyets (1970-2006).

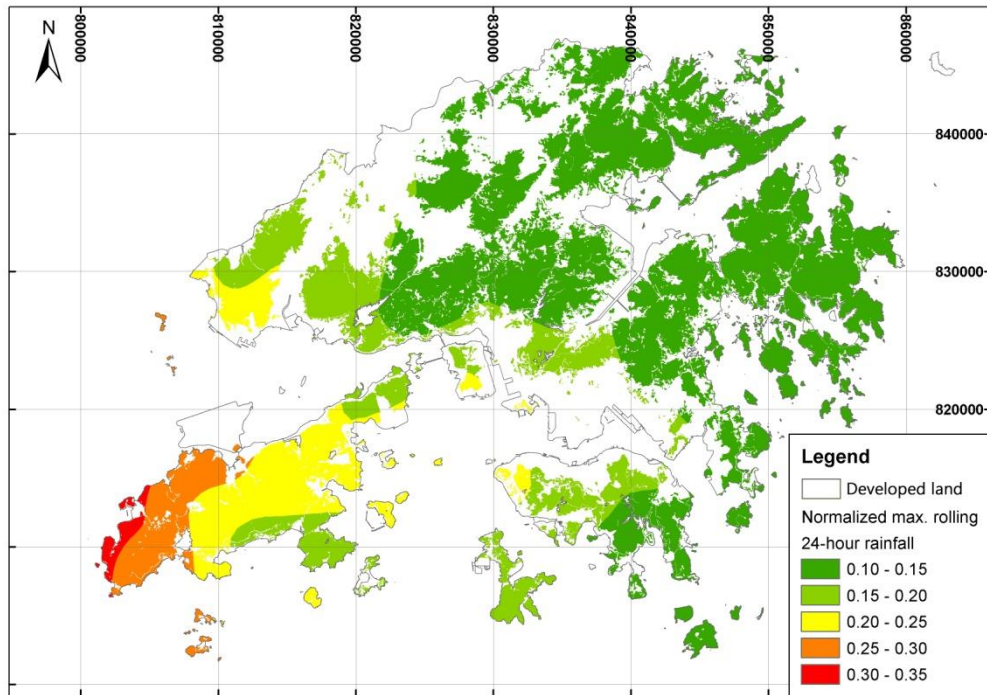


**Fig. 6.** Contours of the year-based normalised maximum rolling 24-hour rainfall over the natural terrain area in 2008.

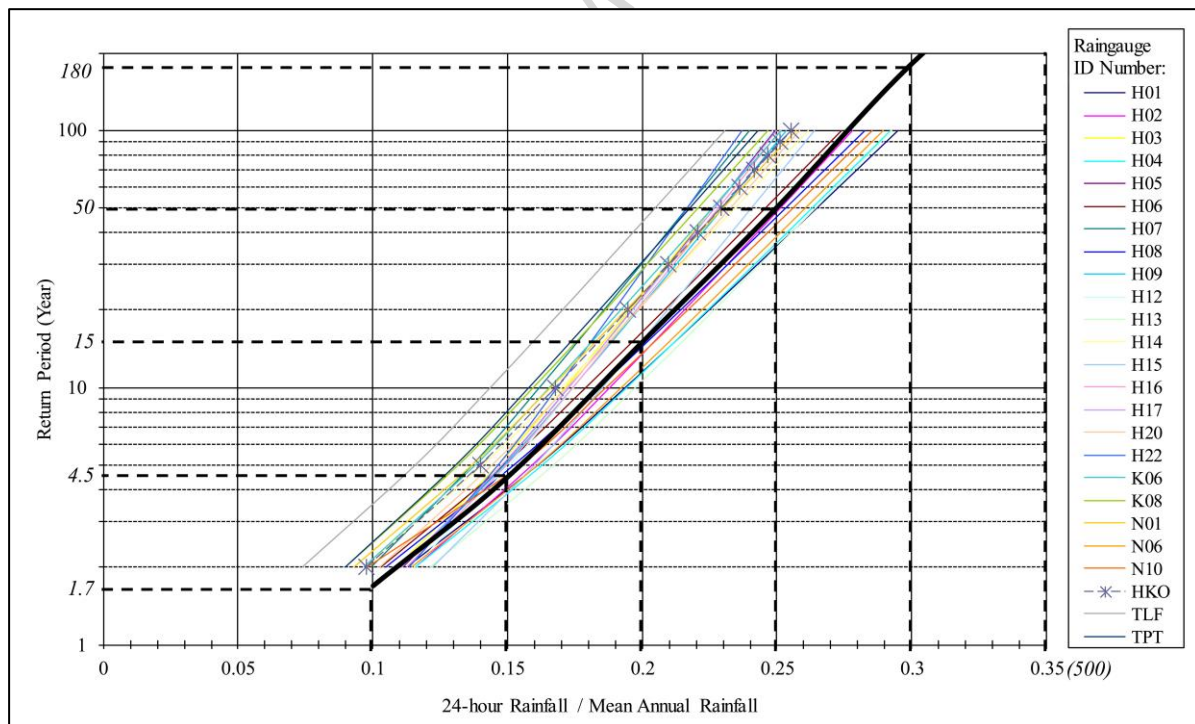


**Fig. 7.** Return periods of normalised maximum rolling 24-hour rainfall at boundaries of rainfall classes 1 to 6.

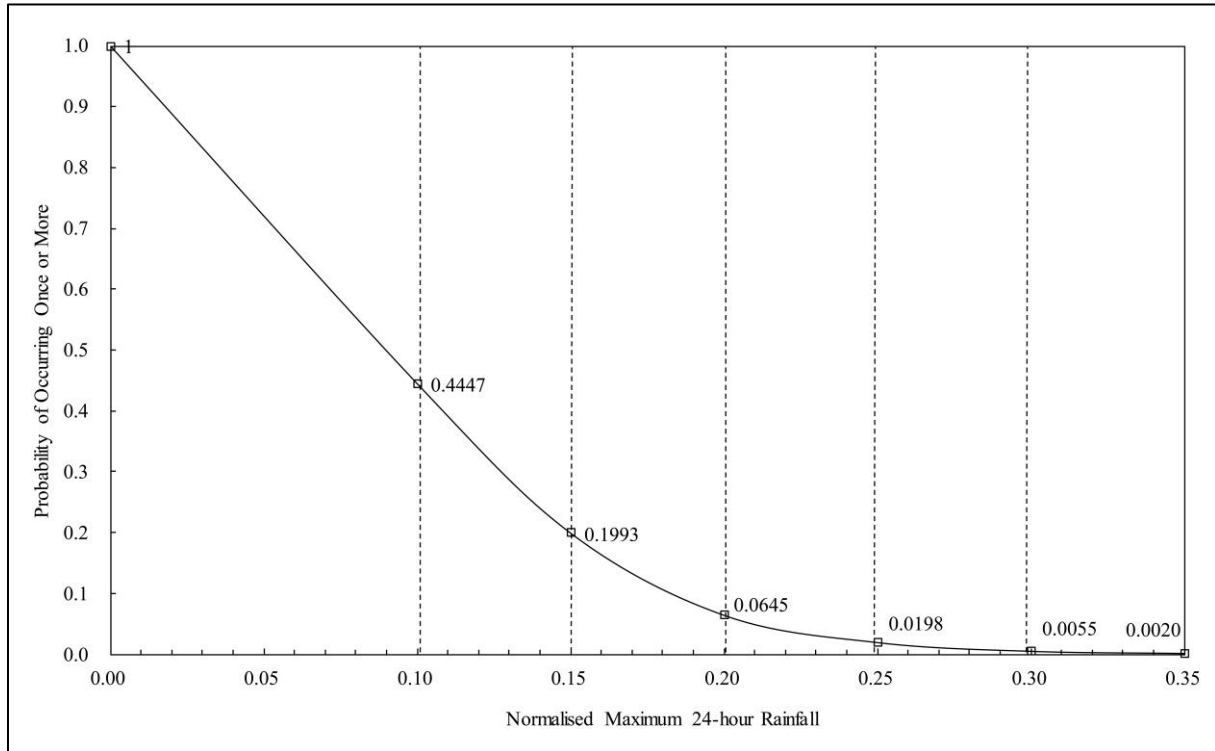


Fig. 8. Probability of occurring once or more of each rainfall class.

Table 2. Assessment of the mean annual frequency of occurrence of rainfall classes.

| $R_{n-24}$ | $T_r$<br>(year) | $P_e$  | Assessment of Probability of Occurrence for Rainfall Scenario |          |          |                  |
|------------|-----------------|--------|---------------------------------------------------------------|----------|----------|------------------|
|            |                 |        | Rainfall Scenario                                             | $P_{es}$ | $T_{rs}$ | $F_{rs}$         |
| 0.10       | 1.7             | 0.4447 | A<br>( $R_{n-24} \leq 0.10$ )                                 | 0.5553   | 1.23     | 0.8130 ( $F_a$ ) |
| 0.20       | 15              | 0.0645 | B<br>( $R_{n-24} > 0.10$ and $\leq 0.20$ )                    | 0.3802   | 2.09     | 0.4785 ( $F_b$ ) |
| 0.30       | 180             | 0.0055 | C<br>( $R_{n-24} > 0.20$ and $\leq 0.30$ )                    | 0.0590   | 16.46    | 0.0608 ( $F_c$ ) |
| 0.35       | 500             | 0.0020 | D<br>( $R_{n-24} > 0.30$ and $\leq 0.35$ )                    | 0.0035   | 281.81   | 0.0035 ( $F_d$ ) |

Note:

$R_{n-24}$  denotes the normalised maximum rolling 24-hour rainfall in a year.

$T_r$  denotes the return period of the corresponding  $R_{n-24}$ .

$P_e$  denotes the probability of exceedance for the corresponding  $R_{n-24}$ .

$P_{es}$  denotes the annual probability of occurring once or more for the corresponding Rainfall Scenario.

$T_{rs}$  denotes the equivalent return period of the corresponding Rainfall Scenario.

$F_{rs}$  denotes the mean annual frequency of occurrence of the corresponding Rainfall Scenario (i.e.  $1/T_{rs}$ ).

The annual theoretical landslide frequency was then calculated by coupling the mean annual frequency of occurrence of rainfall with the storm-based rainfall-landslide susceptibility (Figs. 2 and 3 above) for the four rainfall scenarios to compile the territory-wide terrain-based landslide frequency map. Table 3 summarises the derivation of the annual theoretical landslide frequency, for the four storm-based rainfall scenarios. The annual theoretical landslide frequency for each 5 m x 5 m grid of slope angle class  $i$  and solid geology class  $j$  in the landslide frequency map is  $F_{T,ij}$ , which is calculated as:

$$F_{T,ij} = F_a D_{a,ij} A + F_b D_{b,ij} A + F_c D_{c,ij} A + F_d D_{d,ij} A \dots \dots \dots (1)$$

There are altogether 16 attribute groups in the landslide susceptibility model, arising from the eight slope angle classes (i.e.  $<15^\circ$ ,  $\geq 15^\circ-20^\circ$ ,  $\geq 20^\circ-25^\circ$ ,  $\geq 25^\circ-30^\circ$ ,  $\geq 30^\circ-35^\circ$ ,  $\geq 35^\circ-40^\circ$ ,  $\geq 40^\circ-45^\circ$  and  $\geq 45^\circ$ ) and two solid geology classes (i.e. intrusive and volcanic-cum-sedimentary). The annual theoretical landslide frequency for each grid of each attribute group ranges from the highest value of  $2.3 \times 10^{-4}$  no./year to the lowest value of  $2.8 \times 10^{-7}$  no./year. The annual theoretical landslide frequency according to their corresponding attribute groups is shown in Fig. 9. The grid-based average value of the annual theoretical landslide frequency for all the natural terrain in Hong Kong is  $3.3 \times 10^{-5}$  no./year.

**Table 3.** Derivation of annual theoretical landslide frequency.

| Rainfall Scenario | Normalised 24-hour Rainfall | Theoretical Landslide Frequency (no./year) |
|-------------------|-----------------------------|--------------------------------------------|
| A                 | $\leq 0.10$                 | $F_a D_{a,ij} A$                           |
| B                 | $> 0.10$ and $\leq 0.20$    | $F_b D_{b,ij} A$                           |
| C                 | $> 0.20$ and $\leq 0.30$    | $F_c D_{c,ij} A$                           |
| D                 | $> 0.30$ and $\leq 0.35$    | $F_d D_{d,ij} A$                           |

- Notes:
- (1)  $F_a$ ,  $F_b$ ,  $F_c$  and  $F_d$  are mean annual frequency of occurrence of rainfall for storm-based rainfall scenarios A, B, C and D respectively (see Table 4).
  - (2)  $D_{a,ij}$ ,  $D_{b,ij}$ ,  $D_{c,ij}$  and  $D_{d,ij}$  are storm-based landslide density for rainfall scenarios A, B, C and D respectively, and for a grid of 5 m x 5 m of slope angle class  $i$  and solid geology class  $j$ , based on the rainfall-based landslide susceptibility model (see Fig. 3 and 4).
  - (3)  $A$  is the plan area of a 5 m x 5 m grid (in  $\text{km}^2$ ).

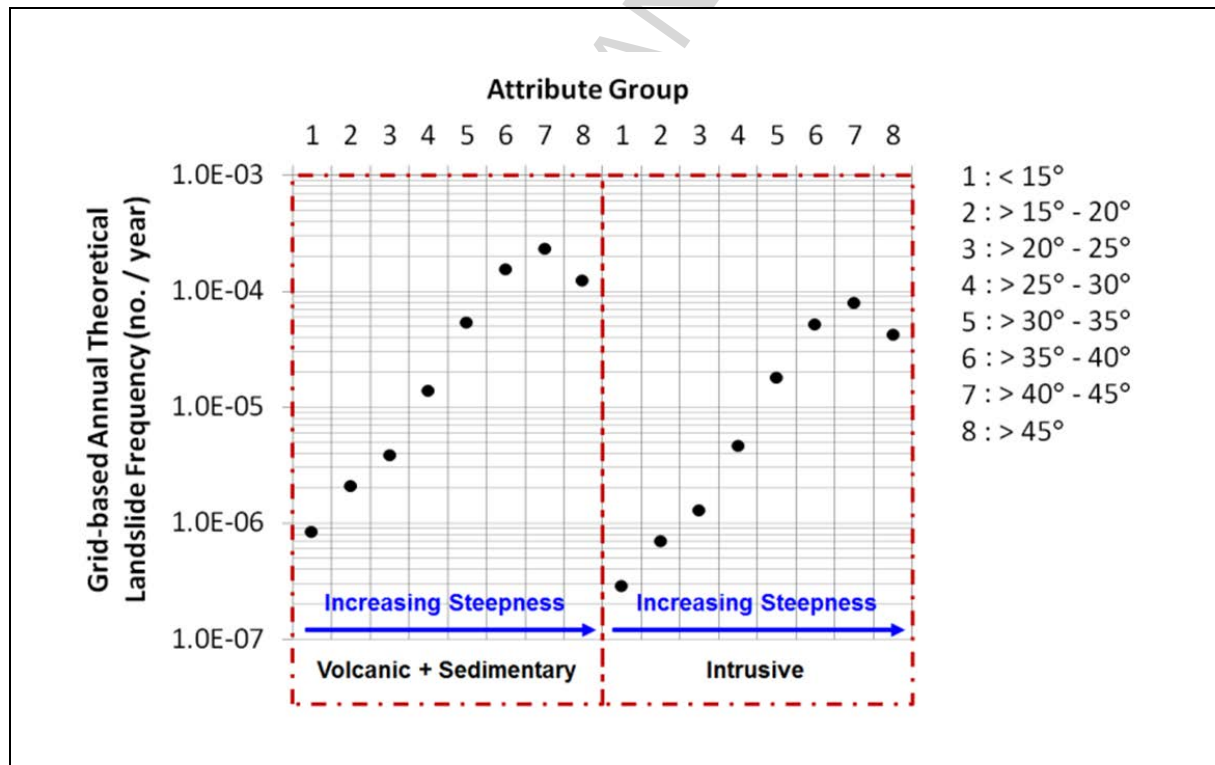


**Fig.9.** Annual theoretical landslide frequency according to attribute groups.

### 3.3 Validation

The performance of the landslide frequency map was evaluated using accuracy statistics and receiver operating characteristic (ROC) curve. Frattini et al. (2010) provided a detailed review on the use of these techniques. Success-rate curve was not applied in evaluating the map performance for the reasons given in Section 6.3. Recent landslides occurred before 1985 were used to evaluate the performance of the landslide frequency map. They were not included in developing the rainfall-based landslide susceptibility model and hence, are statistically independent of the landslide frequency map.

*Accuracy Statistics*

In this technique, accuracy is assessed by comparing the presence and absence of landslides (observed data) within attribute groups that are predicted as relatively stable (predicted positive) and unstable (predicted negative) based on a binary classification of susceptibility (model results). This classification requires a cutoff value of susceptibility that divides the predicted negative terrains (susceptibility less than the cutoff) and predicted positive terrains (susceptibility greater than the cutoff). The comparison of observed data and model results reclassified into two classes is represented through contingency tables. An example of a generic contingency table is shown in Table 4. Accuracy statistics assess the model performance by combining correctly and incorrectly classified positives and negatives.

Susceptibility classes I and II in the landslide frequency map (corresponding to areas with an above-average theoretical landslide frequencies) were classified as predicted positive and classes III, IV and V as predicted negative (corresponding to areas with an average theoretical landslide frequencies or below).

**Table 4.** Contingency table used for landslide model evaluation.

|           |          | Observed                          |                                   |
|-----------|----------|-----------------------------------|-----------------------------------|
|           |          | Positive                          | Negative                          |
| Predicted | Positive | True Positive (TP)                | False Positive (FP)               |
|           | Negative | False Negative (FN)               | True Negative (TN)                |
|           |          | Sensitivity<br>= $TP / (TP + FN)$ | Specificity<br>= $TN / (FP + TN)$ |

*Receiver Operating Characteristic Curve*

In this technique, the susceptibility classes are arranged from the highest to the lowest. By considering a range of possible cutoff values, pairs of sensitivity and (1-specificity) are derived and plotted with the former on the y-axis and latter on the x-axis. The area under curve (AUC) can be used as a metric to assess the overall quality of a model: the larger the area, the best the performance of the model over the whole range of possible cutoffs. A value of 0.5 indicates a random result, a value approaching 1.0 indicates good prediction. As compared to the contingency table, the application of ROC curve do not require a priori cutoff value and the performance of a landslide susceptibility map is assessed throughout the entire range of cutoff values.

*Success-rate Curve*

A success-rate curve represents the percentage of correctly classified objects (i.e. terrain units) on the y-axis, and the percentage of area classified as positive terrains on the x-axis. In the grid-cell units where landslides correspond to single grid cells and all the terrain units have the same area, the y-axis corresponds to the value of sensitivity, analogous with the ROC space, and the x-axis corresponds to the percentage of units classified as positive (i.e.  $(TP + FP) / (TP + FP + TN + FN)$  in Table 4). When FP and TN are significantly larger than TP and FN (i.e. the observed failure rate is low), the x-axis corresponds to the value of 1-specificity, analogous with the ROC space, as in the present study. Therefore, for this study, the success-rate curve thus coincides with the ROC curve. It should also be noted that the high FP to TP ratio of the present study does not necessarily constitute an adverse condition for landslide susceptibility assessment (Carrara et al 2008). Instead, the ratio reflects a low number of failures in the predicted positive terrains throughout the observation period and in fact represents a low actual failure probability. This ratio should not be used to indicate how good a landslide susceptibility model performs.

#### 4 Terrain-based Landslide Frequency Map

A terrain-based landslide frequency map was compiled based on the annual theoretical landslide frequency.

The map is a digital map on a GIS platform showing the annual theoretical landslide frequency for every grid of 5 m x 5 m on the natural terrain. The chosen 5 m by 5 m resolution appears to be an appropriate scale for the present analysis. This grid size is comparable with the scale of majority of the natural terrain landslide source areas. In the map, the annual theoretical landslide frequencies are categorised into five classes to represent their relative levels of terrain susceptibility to landslide, each shown in a different colour (Table 5). Fig. 10 shows a typical map layout. The area distribution of the five susceptibility classes is summarised in Table 6.

**Table 5.** Susceptibility class and colour codes of grid-based annual theoretical landslide frequency.

| Susceptibility Class | Colour Code | Grid-based Annual Theoretical Landslide Frequency (no./year) |
|----------------------|-------------|--------------------------------------------------------------|
| I                    | Yellow      | $> 1.0 \times 10^{-4}$                                       |
| II                   | Light Blue  | $> 5.0 \times 10^{-5} - 1.0 \times 10^{-4}$                  |
| III                  | Dark Blue   | $> 1.0 \times 10^{-5} - 5.0 \times 10^{-5}$                  |
| IV                   | Light Green | $> 1.0 \times 10^{-6} - 1.0 \times 10^{-5}$                  |
| V                    | Dark Green  | $< 1.0 \times 10^{-6}$                                       |

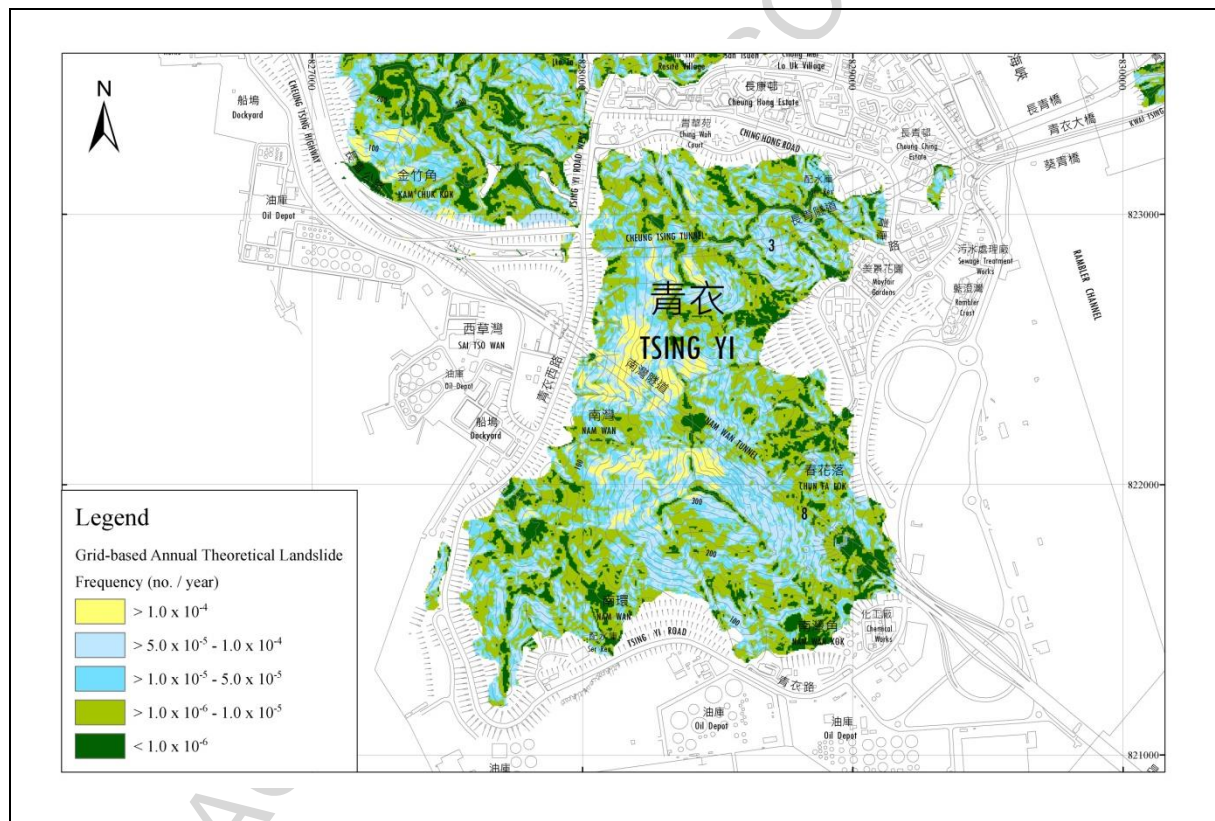


**Fig. 10.** Typical map layout and legend.

**Table 6.** Area distribution of susceptibility classes.

| Susceptibility Class | Area (km <sup>2</sup> ) | Percentage Area |
|----------------------|-------------------------|-----------------|
| I                    | 75.2                    | 11.4%           |
| II                   | 113.9                   | 17.3%           |
| III                  | 149.1                   | 22.7%           |
| IV                   | 218.2                   | 33.2%           |
| V                    | 101.5                   | 15.4%           |

## 5 Map Performance

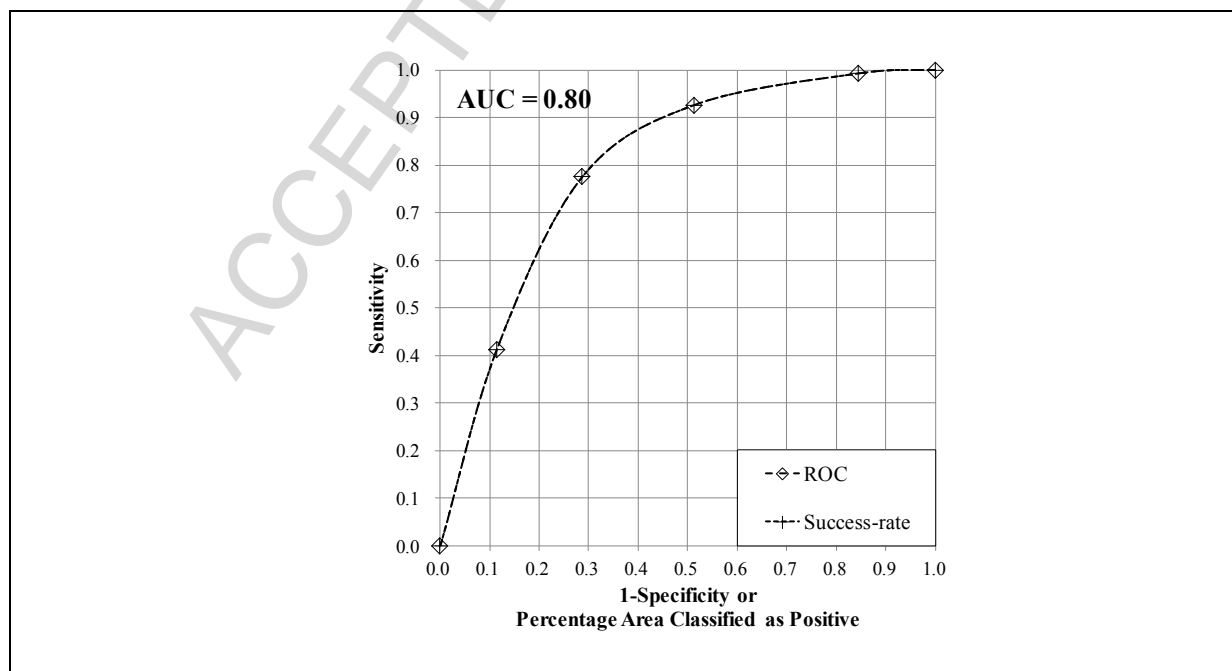
The performance of the landslide frequency map was evaluated using accuracy statistics and receiver operating characteristic (ROC) curve. Frattini et al. (2010) provided a detailed review on the use of these techniques. Success-rate curve was not applied in evaluating the map performance for the reasons given in Section 6.3. Recent landslides occurred before 1985 were used to evaluate the performance of the landslide frequency map. They were not included in developing the rainfall-based landslide susceptibility model and hence, are statistically independent of the landslide frequency map.

Table 7 gives the contingency tables that compare the presence and absence of landslides within the predicted positive and negative attribute groups. There are about 78% of recent landslides fall within susceptibility classes I and II in the landslide frequency map. About 71% of pixels with no observed landslides are classified as susceptibility classes III, IV and V have no landslides.

The ROC curve of the map is shown in Fig. 11. The value of AUC achieved is 0.80. It shows that there is a reasonably high degree of agreement between observed data and model results. The results indicate that the map is consistent with the observed data to give reasonable prediction of both landslide occurrence and non-occurrence considering the entire possible range of cutoff values.

**Table 7.** Validation results using accuracy statistics.

|           |          | Observed                |                         |
|-----------|----------|-------------------------|-------------------------|
|           |          | Positive                | Negative                |
| Predicted | Positive | 5846                    | 83139914                |
|           | Negative | 1693                    | 206235535               |
|           |          | Sensitivity<br>= 77.54% | Specificity<br>= 71.27% |



**Fig. 11.** ROC and Success-rate curve of the landslide frequency map.

Hungr (2016) proposed, with an example shown, a simple and direct approach to validate a landslide susceptibility map in which errors (residuals) of density estimation (in terms of landslide area per km<sup>2</sup>) are presented directly, for all the susceptibility class of the map. Details about how the approach works are not repeated here. Table 8 shows the results of the proposed analysis of the landslide frequency map in this study.

The residual error represented by the difference between corrected and observed susceptibility percentages for each class is very small for the following reasons:

- (a) Natural terrain in Hong Kong has a relatively low failure frequency that ranges from 10<sup>-4</sup> to 10<sup>-7</sup> number of landslides per year per 5 m grid. Any errors of density estimation are insignificant.
- (b) The landslide frequency map provides classification of landslide susceptibility that is consistent with the observed data.
- (c) The predicted landslide frequency of each landslide susceptibility class is realistic with the consideration of rainfall as the key causal factor that represents closely the controlling physical phenomenon of occurrence of rainfall-induced shallow landslides in Hong Kong.

**Table 8.** Results of validation analysis proposed by Hungr (2016).

| Class | Terrain Area       |        | Observed Landslides |                     |                        | Predicted Landslides |                     |                        | Corrected Landslides <sup>(3)</sup> |                   |         | Error  |
|-------|--------------------|--------|---------------------|---------------------|------------------------|----------------------|---------------------|------------------------|-------------------------------------|-------------------|---------|--------|
|       |                    |        | Landslide           | Area <sup>(1)</sup> | Density <sup>(2)</sup> | Landslide            | Area <sup>(1)</sup> | Density <sup>(2)</sup> | Landslide                           | Area              | Density |        |
|       | (km <sup>2</sup> ) | (%)    | (no.)               | (m <sup>2</sup> )   | (%)                    | (no.)                | (m <sup>2</sup> )   | (%)                    | (no.)                               | (m <sup>2</sup> ) | (%)     | (%)    |
| I     | 97.19              | 14.02  | 2185                | 156227              | 0.16%                  | 6414.4               | 458630              | 0.47%                  | 2624                                | 187584            | 0.19%   | 0.03%  |
| II    | 159.45             | 23.00  | 2513                | 179679              | 0.11%                  | 5262.0               | 376230              | 0.24%                  | 2152                                | 153882            | 0.10%   | -0.01% |
| III   | 219.58             | 31.67  | 1163                | 83154               | 0.04%                  | 2898.5               | 207242              | 0.09%                  | 1186                                | 84764             | 0.04%   | 0.00%  |
| IV    | 185.45             | 26.75  | 252                 | 18018               | 0.01%                  | 408.0                | 29171               | 0.02%                  | 167                                 | 11931             | 0.01%   | 0.00%  |
| V     | 31.61              | 4.56   | 18                  | 1287                | 0.00%                  | 7.0                  | 497                 | 0.00%                  | 3                                   | 203               | 0.00%   | 0.00%  |
| Total | 693.28             | 100.00 | 6131                | 438365              |                        | 14990                | 1071771             |                        | 6131                                | 438365            |         |        |

- Notes:
- (1) Landslide area is calculated based on the mean source area of the recent landslides in the Enhanced Natural Terrain Landslide Inventory.
  - (2) Density is the quotient of the landslide area within a susceptibility class divided by the terrain area within the same class.
  - (3) Data in columns under “corrected landslides” are obtained by multiplying the corresponding data in columns under “predicted landslides” by a correction ratio, such that their total equal to that of the observed landslides.

## 6 Discussions

### 6.1 Key Observations for Landslide Frequency Map

The landslide frequency map was built on the findings of the rainfall-based landslide susceptibility analysis. The analysis assessed average landslide response to rainfall for each of the 16 groups of terrain, in terms of theoretical landslide density. In other words, landslide response is shared across the entire terrain of the same attribute group, for a given rainfall scenario. For terrain in the same attribute group, areas with and without past rainfall experience have the same terrain susceptibility. As a result, terrain susceptibility as indicated in the landslide frequency map is independent of past rainfall experience.

As it is independent of past rainfall experience, the landslide frequency map could be used as a tool for forward prediction on the potential of landslide occurrence for a given rainfall scenario in the future, which may be calculated based on the theoretical landslide frequency. At a global scale, it fills the gap in the current practice of hazard evaluation, which refers largely to record of past landslides, and opens up the source of potentially problematic natural hillsides. The map should however not be used for terrain evaluation and assessment at

site-specific scale because of a lack of adequate resolution to duly account for site-specific terrain conditions. It may however be a useful supplementary reference.

One of the major assumption in the model is that the frequency of occurrence of each rainfall class is stationery. With climate change, the frequency of extreme rainfall events extreme weather is expected to increase (Lee et al, 2011). Sensitivity analysis can be performed by coupling the rainfall-based susceptibility model with different sets of frequencies of rainfall classes taking into account the expected changes.

The current model is based on four rainfall classes. Should there are more abundant data in both spatial and temporal manner, there may be a room to introduce more rainfall classes and thus enhancing the resolution of the calculated landslide frequency with a view to further enhancing the map performance.

## 6.2 Comments on Receiver Operating Characteristic Curves

The application of ROC curves does not require a priori cutoff value and the performance of a landslide susceptibility map is assessed throughout the entire range of cutoff values. Nevertheless, the study of a variety of ROC curves of different cases revealed that the value of AUC of a ROC curve is sensitive to, for example, the approach of calculating AUC, the percentage of pixels with and without landslides (this also depends on the observation period) and map classification. Two illustrations, amongst many other possibilities, are shown below to demonstrate that the value of AUC of a ROC curve is quite sensitive:

(a) Scenario 1. A slight change in the percentage of pixels with landslides for the lowest susceptibility class from 10% to 0% and for the highest susceptibility classes from 90% to 100%, while keeping the percentage of pixels with landslides for other susceptibility classes unchanged, improve the value of AUC from 0.76 to 0.82 (Table 9(a) & (b) respectively). In practice, both models produce equally good results.

(b) Scenario 2. Separating the pixels without landslides from the lowest susceptibility class to a further lower class improves the value of AUC from 0.77 to 0.82. (Table 9(c) & (b) respectively).

**Table 9.** Hypothetical scenarios.

(a) Scenario 1(a)

| Susceptibility Class | No. of Pixels | No. of Pixels with Landslides | No. of Pixels without Landslides | AUC  |
|----------------------|---------------|-------------------------------|----------------------------------|------|
| I (the highest)      | 767           | 690                           | 77                               | 0.76 |
| II                   | 3,550         | 2,840                         | 710                              |      |
| III                  | 7,318         | 3,659                         | 3,659                            |      |
| IV                   | 18,471        | 3,694                         | 14,777                           |      |
| V (the lowest)       | 7,668         | 767                           | 6,901                            |      |

(b) Scenario 1(b)

| Susceptibility Class | No. of Pixels | No. of Pixels with Landslides | No. of Pixels without Landslides | AUC  |
|----------------------|---------------|-------------------------------|----------------------------------|------|
| I (the highest)      | 767           | 767                           | 0                                | 0.82 |
| II                   | 3,550         | 2,840                         | 710                              |      |
| III                  | 7,318         | 3,659                         | 3,659                            |      |
| IV                   | 18,471        | 3,694                         | 14,777                           |      |
| V (the lowest)       | 7,668         | 0                             | 7,668                            |      |

(c) Scenario 2

| Susceptibility Class | No. of Pixels | No. of Pixels with Landslides | No. of Pixels without Landslides | AUC  |
|----------------------|---------------|-------------------------------|----------------------------------|------|
| I (the highest)      | 767           | 767                           | 0                                | 0.77 |
| II                   | 3,550         | 2,840                         | 710                              |      |
| III                  | 7,318         | 3,659                         | 3,659                            |      |
| IV (the lowest)      | 26,139        | 3,694                         | 22,445                           |      |

The above observations are less evident when the percentage of pixels without landslides is large, such as that in the present study. It appears that the model results of the present study are not sensitive to any changes in either the map classification or the observed data. In addition, when calculating AUC, one may choose to calculate the AUC of a fitted curve through the discrete points of a ROC curve or simply calculate the area under the continuous line joining the discrete points. The fewer the divisions in the map classification, the larger is the difference between the two approaches. In most cases, this would be a concern when a landslide susceptibility map has only three to four divisions of landslide susceptibility.

Because of the sensitivity of the AUC, the value of AUC should only be taken as a rough indication of how good a landslide susceptibility map performs in landslide prediction. When comparing different model results using the values of AUC of the respective ROC curves, the sensitivity of the values of AUC should be duly accounted for and the significance of AUC in evaluating how good a landslide susceptibility map performs in landslide prediction should not be overly emphasised. It is always important to look into the data and evaluate, for example, the percentage of pixels with and without landslides in each susceptibility class, in order to determine whether the landslide susceptibility maps produce logical results and whether one map is better than the others in terms of landslide prediction.

### 6.3 Comments on Success-rate Curves

As to success-rate curves, although its application does not require a priori cutoff value and the performance of a landslide susceptibility map is assessed throughout the entire range of cutoff values, alike ROC curves, they have the following distinct limitations:

(a) Success-rate curves represent the percentage of correctly classified objects (i.e. terrain units) on the y-axis, and the percentage of positive terrains on the x-axis. The capability of the map to predict absence of landslides is not considered.

(b) Success-rate curves are sensitive to the initial proportion of positive and negative terrains (Frattini et al 2010), as they consider the percentage of positive terrains of a map on the x-axis. The application of success-rate curve to an area with a low degree of hazard gives better result than application to an area with a high hazard, even if the quality of the classifications are exactly the same. Fig. 12 explains this observation with two hypothetical study areas. The ROC curves rightly indicate that the performance of the susceptibility map have similar performance for the two study areas as the two ROC curves are in close resemblance of each other with the area under curve (AUC) of 0.78 and 0.81 for high hazard area and low hazard area respectively. On the other hand, the success-rate curve indicates that there is a drop in performance of the map in the high hazard area with an AUC of 0.65, as compared to 0.77 of the low hazard area. It indicates that the application of success-rate curve to an area with a low degree of hazard gives better result than application to an area with a high hazard, even if the quality of the classifications are exactly the same. The percentage of positive terrains indeed represents the predicted failure probability of the area and is irrelevant to how good a landslide susceptibility map performs. A landslide susceptibility map should receive appropriate credibility as long as it rightly “catches” as many as possible actual landslides. The distribution of susceptibility classes in a map should be irrelevant.

(c) Confining pixels of the highest susceptibility to those areas with landslides in a landslide susceptibility map, i.e. to reduce the percentage of positive terrains as far as possible, would greatly improve the AUC of the success-rate curve. This is similar to what may be done to improve the AUC of a ROC curve.

(d) Because of the above, the reliability of the AUC of a success-rate curve should be treated with caution when it is used as a sole indicator to consider how good a landslide susceptibility map performs in landslide prediction.

## **7 Conclusions**

The digital landslide frequency map building on the findings of the rainfall-based landslide susceptibility analysis has been produced using GIS technology. It is currently for internal use by the GEO to support the review of landslide susceptibility of natural terrain in Hong Kong. A number of techniques were applied to evaluate the landslide frequency map and the validation shows that the map is highly consistent with the observed data for both presence and absence of landslides. Areas for improvement are constantly identified with a view to further improving the predictability of the landslide frequency map.

## **8 Acknowledgements**

This paper is published with the permission of the Head of the Geotechnical Engineering Office and the Director of Civil Engineering and Development, Government of the Hong Kong Special Administrative Region.

**Study Area A : High Hazard Area**Susceptibility Map

|   |   |   |   |   |
|---|---|---|---|---|
| 1 | 1 | 1 | 1 | 2 |
| 1 | 1 | 1 | 2 | 2 |
| 1 | 1 | 2 | 2 | 3 |
| 1 | 2 | 2 | 3 | 4 |
| 2 | 2 | 3 | 4 | 5 |

Number of pixels with landslide observed

|     |     |     |     |     |
|-----|-----|-----|-----|-----|
| 300 | 300 | 300 | 300 | 150 |
| 300 | 300 | 300 | 150 | 150 |
| 300 | 300 | 150 | 150 | 75  |
| 300 | 150 | 150 | 75  | 30  |
| 150 | 150 | 75  | 30  | 10  |

**Study Area B : Low Hazard Area**Susceptibility Map

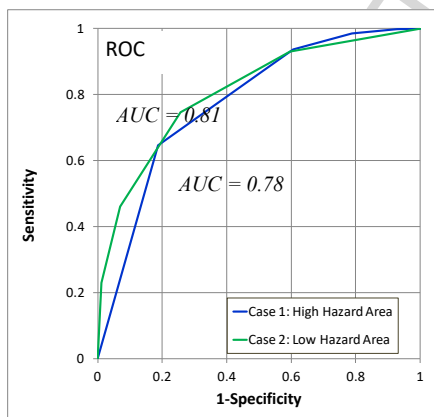
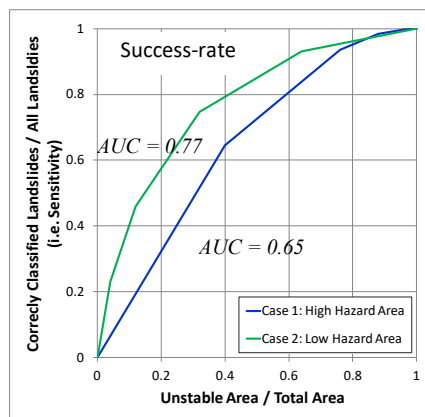
|   |   |   |   |   |
|---|---|---|---|---|
| 1 | 2 | 3 | 4 | 5 |
| 2 | 3 | 3 | 4 | 5 |
| 3 | 3 | 4 | 4 | 5 |
| 4 | 4 | 4 | 4 | 5 |
| 5 | 5 | 5 | 5 | 5 |

Number of pixels with landslide observed

|     |     |    |    |    |
|-----|-----|----|----|----|
| 300 | 150 | 75 | 30 | 10 |
| 150 | 75  | 75 | 30 | 10 |
| 75  | 75  | 30 | 30 | 10 |
| 30  | 30  | 30 | 30 | 10 |
| 10  | 10  | 10 | 10 | 10 |

*Notes:*

1. Each cell is assumed to represent 20 pixels by 20 pixels.
2. "1" denotes susceptibility class I (the most susceptible), while "5" denotes susceptibility class V (the least susceptible).

**ROC Curves****Success-rate Curves**

**Fig 12.** Hypothetical study areas for comparison of ROC curves and success-rate curves.

## References

- Baum, R.L., Savage, W.Z. and Godt, J.W., 2002. *TRIGRS - A Fortran Program for Transient Rainfall Infiltration and Grid Based Regional Slope Stability Analysis*. Open file report 02-424: Colorado, USA, U.S. Department of the Interior and U.S. Geological Survey.
- Brand, E.W., Premchitt, J. and Phillipson, H.B., 1984. Relationship between rainfall and landslides in Hong Kong. *Proceedings of the Fourth International Symposium on Landslides*, Toronto, vol. 1, pp 377-384.
- Bui, D.T., Tuan, T.A., Hoang, N.D., Thanh, N.Q., Hguyen, D.B., Liem, N.V. and Pradhan, B., 2016. Spatial prediction of rainfall-induced landslides for the Lao Cai area (Vietnam) using a hybrid intelligent approach of least squares support vector machines inference model and artificial bee colony optimization. *Landslides*, doi:10.1007/s10346-016-0711-9.
- Carrara, A., Crosta, G. and Frattini, P. 2008., Comparing models of debris-flow susceptibility in the alpine environment. *Geomorphology*, 94 (3-4), pp 353-378.
- Casadei, M., Dietrich, W.E. and Miller, N.L., 2003. Testing a model for predicting the timing and location of shallow landslide initiation on soil mantled landscapes. *Earth Surface Processes and Landforms*, 28 (9), pp 925-950.
- Chan, R.K.S., Pang, P.L.R. and Pun, W.K., 2003. Recent developments in the Landslip Warning System in Hong Kong. *Proceedings of the Asian Technical Committee (ATC 3) Workshop on Rain-induced Landslides*, Hong Kong, vol. 3, pp 219-224.
- Chan, C.H.W., Ting, S.M. and Wong, A.C.W., 2012. *Development of Natural Terrain Landslip Alert Criteria (Special Project Report No. SPR 1/2012)*. Geotechnical Engineering Office, Hong Kong, 68 p.
- Cornell, C.A., 1968. Engineering seismic risk analysis. *Bulletin of the Seismological Society of America*, 58 (5), 1583-1606.
- Corominas, J., Van Westen, C., Frattini, P., Cascini, L., Malet, J.P., Fotopoulou, S., Catani, F., Van Den Eeckhaut, M., Mavrouli, O., Agliardi, F. and Pitilakis, K., 2014. Recommendations for the quantitative analysis of landslide risk. *Bulletin of engineering geology and the environment*, 73(2), 209-263.
- Dai, F.C. and Lee, C.F., 2002. Terrain-based mapping of landslide susceptibility using a geographic information system: a case study. *Canadian Geotechnical Journal*, Vol. 38, pp 911-923.
- Evans, N.C. and King, J.P., 1998. *The Natural Terrain Landslide Study: Debris Avalanche Susceptibility (Technical Note TN 1/98)*. Geotechnical Engineering Office, Hong Kong, 96 p.
- Frattini, P., Crosta, G. and Carrara, A., 2010. Techniques for evaluating the performance of landslide susceptibility models. *Engineering Geology*, 111, pp 62-72.
- GEO, 1996. *Report on the Shum Wan Road landslide of 13 August 1995 vol. 2 : findings of the landslide investigation*. Geotechnical Engineering Office, Hong Kong, 51 p.
- GEO, 2017. *Detailed Study of the 21 May 2016 Landslide on the Natural Hillside above Slope No. 8SE-A/F34 at Sai Kung Sai Wan Road, Sai Kung (Landslide Study Report No. LSR 3/2017)*. Geotechnical Engineering Office, Hong Kong.
- Godt, J.W., Baum, R.L., Savage, W.Z., Salciarini, D., Schulz, W.H. and Harp, E.L., 2008. Transient deterministic shallow landslide modeling: Requirements for susceptibility and hazard assessments in a GIS framework. *Engineering Geology*, 102(3), pp 214-226.
- Guzzetti, F., Carrara, A., Cardinali, M and Reichenbach, P., 1999. Landslide hazard evaluation: a review of current techniques and their application in a multi-scale study, Central Italy. *Geomorphology*, 31, pp 181-216.
- Hungr, O., Evans, S.G. and Hazzard, J., 1999. Magnitude and frequency of rock falls and rock slides along main transportation corridors southwestern British Columbia. *Canadian Geotechnical Journal*, 35, pp 224-238.
- Hungr, O., 2016. A review of landslide hazard and risk assessment methodology. *Proceedings of the 12<sup>th</sup> International Symposium on Landslides*, Naples, Italy, pp 3-27.
- IUGS Working Group on Landslides, Committee on Risk Assessment, 1997. Quantitative risk assessment for slopes and landslides - The state of the art. *Proceedings of the Landslide Risk Workshop*, IUGS Working Group on Landslides, Honolulu, pp 3-12.
- Iverson, R.M., 2000. Landslide triggering by rain infiltration. *Water Resources Research*, 36(7), pp 1897-1910.
- Ko, F.W.Y., 2005. *Correlation between Rainfall and Natural Terrain Landslide Occurrence in Hong Kong (GEO Report No. 168)*. Geotechnical Engineering Office, Hong Kong, 77 p.
- Ko, F.W.Y. and Lo, F.L.C., 2016. Rainfall-based landslide susceptibility analysis for natural terrain in Hong Kong - A direct stock-taking approach. *Engineering Geology*, 215 (2016), 95-107.
- Lari, S., Frattini, P., & Crosta, G.B., 2014. A probabilistic approach for landslide hazard analysis. *Engineering Geology*, 182, 3-14.
- Lee, T.C., Chan, K.Y., Chan, H.C. and Kok, M.H., 2011. Projections of extreme rainfall in Hong Kong in the 21<sup>st</sup>

- Century. *Journal of Meteorological Research*, 25(6), 691-709.
- Lee, C.F., Huang, C.M., Tsao, T.C., Wei, L.W., Huang, W.K., Cheng, C.T. and Chi, C.C., 2016. Combining rainfall parameter and landslide susceptibility to forecast shallow landslide in Taiwan. *Geotechnical Engineering Journal of the SEAGS & AGSSEA*, 47 (2), pp. 72-82.
- McMackin, M.R., Clahan, K.B. & Dee, S.M., 2009. A unique deep-seated debris slide near Shek Pik reservoir associated with the June 7th 2008, black rain storm. *Proceedings of the HKIE Geotechnical Division Annual Seminar 2009*. Geotechnical Division, the Hong Kong Institution of Engineers, pp 79-84.
- Parry, S. & Campbell, S.D.G. 2003. *A Large Scale Very Slow Moving Natural Terrain Landslide in the Leung King Valley (Geological Report No. GR 2/2003)*. Geotechnical Engineering Office, Hong Kong, 60 p.
- Roberds, W., 2005. Estimating temporal and spatial variability and vulnerability. *Landslide Risk Management*. Edited by Hungr, O., Fell, R., Couture R. and Eberhardt, E. Taylor & Francis, London, pp 129-158.
- Simonie, S., Zanotti, F., Bertoldi, G. and Rigon, R., 2008. Modelling the probability of occurrence of shallow landslides and channelised debris flows using GEOtop-FS. *Hydrological Processes*, 22 (4), pp 532-545.
- Van Den Eeckhault, M., Reichenbach, P., Guzzetti, F., Rossi, M. and Poesen, J., 2009. Combined landslide inventory and susceptibility assessment based on different mapping units: an example from the Flemish Ardennes, Belgium. *Natural Hazards and Earth System Sciences*, no. 9, pp 507-521.
- Van Westen, C.J., Castellanos Abella, E.A. and Sekhar, L.K., 2008. Spatial data for landslide susceptibility, hazards and vulnerability assessment: an overview. *Engineering Geology*, 102 (3-4), pp 112-131.
- Wong, H.N., 2009. Rising to the challenges of natural terrain landslides. *HKIE Geotechnical Division Annual Seminar 2009*, Hong Kong, 15-53.
- Wong, H.N. and Ko, F.W.Y., 2006. Evolution of slope engineering practice and landslide risk management in Hong Kong. *Proceedings of the International Conference on Slopes*, Malaysia 2006, Kuala Lumpur, Malaysia, pp 269-311.
- Wong, A.C.W., Ting, S.M., Shiu, Y.K. and Ho, K.K.S., 2013. Latest Developments of Hong Kong's Landslip Warning System. *Proceedings of the World Landslide Forum 3*, Vol. 2, pp 613-618.
- Wong, H.N., Ko, F.W.Y. and Hui, T.H.H., 2006. *Assessment of Landslide Risk of Natural Hillsides in Hong Kong (GEO Report No. 191)*. Geotechnical Engineering Office, Hong Kong, 117 p.
- Wong, H.N., Shum, W.W.L. and Ko, F.W.Y., 2004. *Assessment of Natural Terrain Landslide Risk on the Planned Development in Ling Pei, Lantau (Advisory Report No. ADR 4/2004)*. Geotechnical Engineering Office, Hong Kong, 174 p.

**From landslide susceptibility to landslide frequency: a territory-wide study in Hong Kong**Highlights

- A territory-wide landslide frequency map was for natural hillside in Hong Kong.
- Landslide frequency established considering the probability of different rainfall scenarios.
- The performance of the map has been validated against historical landslide data.
- There is a reasonably high degree of agreement between observed data and the map.

ACCEPTED MANUSCRIPT



Figure 1

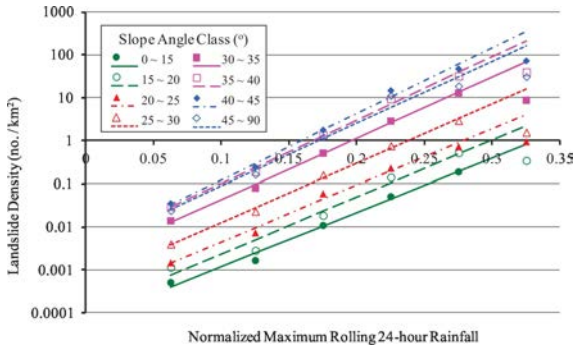


Figure 2

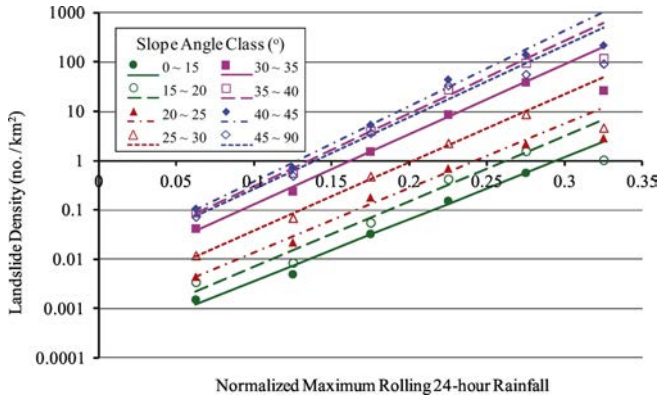


Figure 3

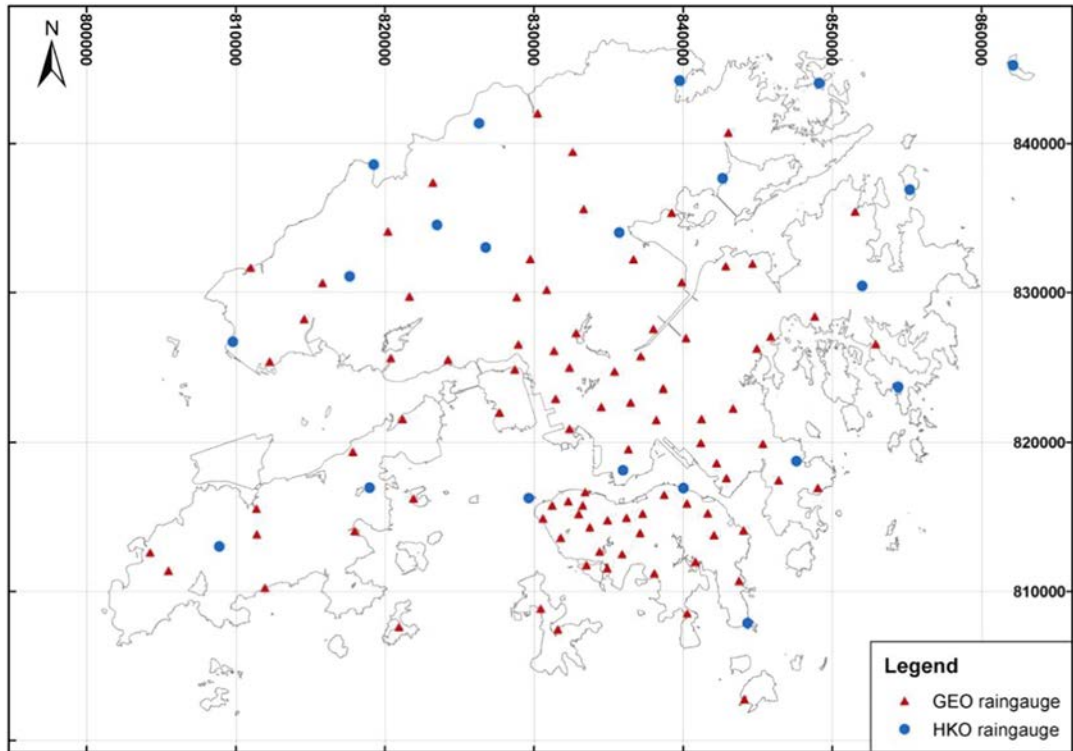


Figure 4

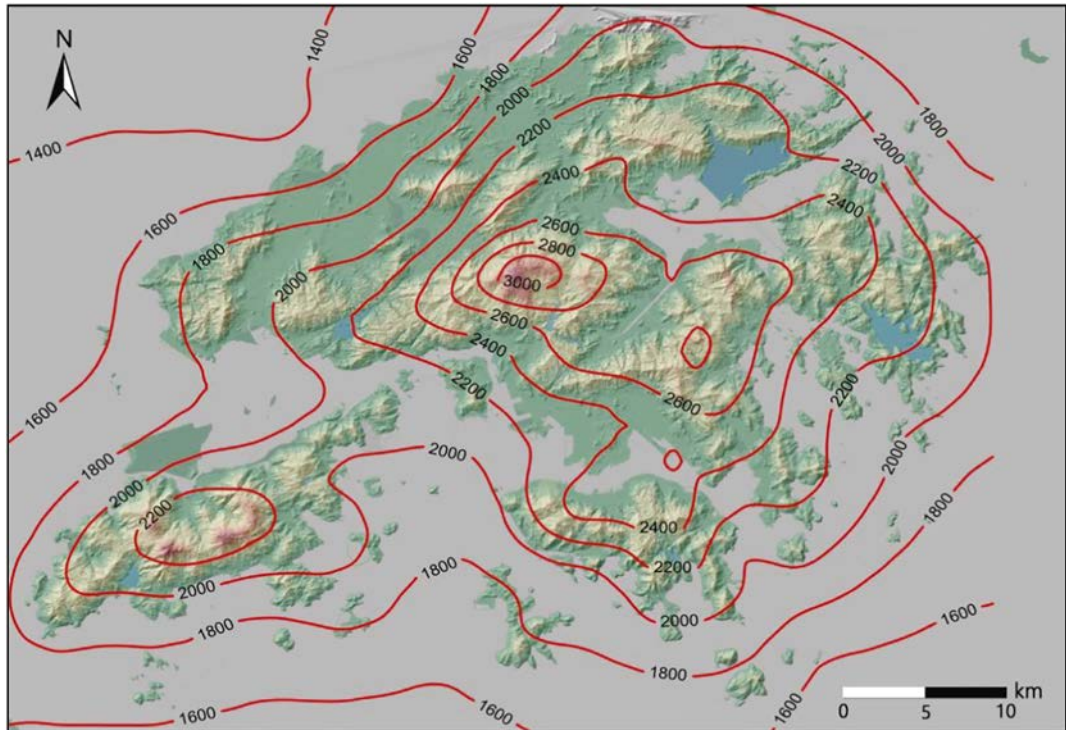


Figure 5

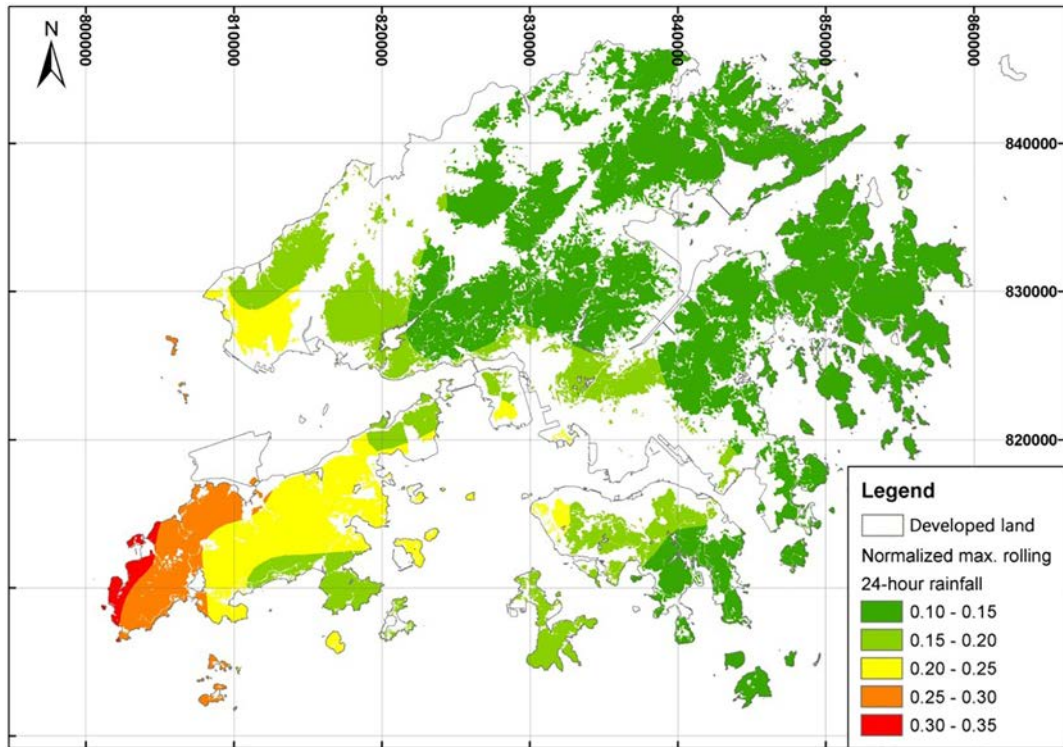


Figure 6

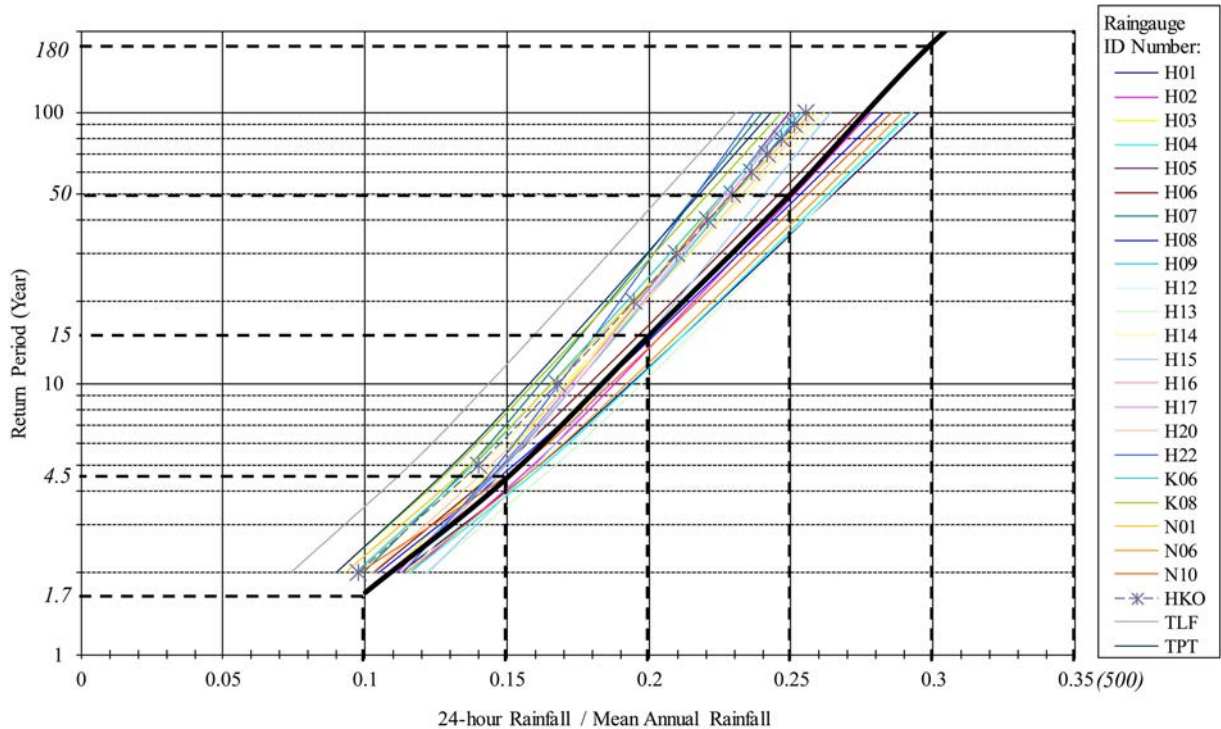


Figure 7

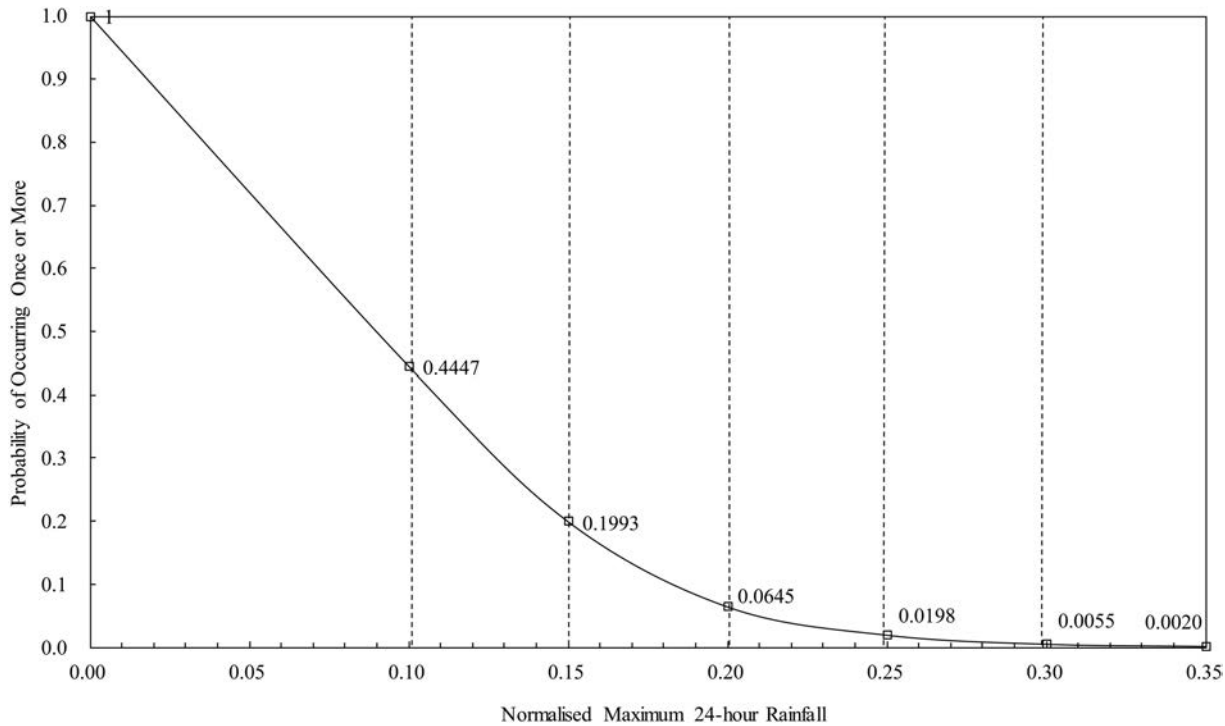


Figure 8

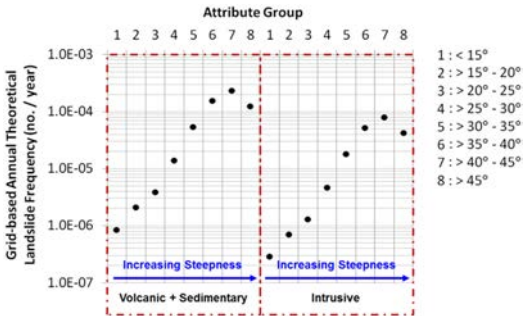


Figure 9



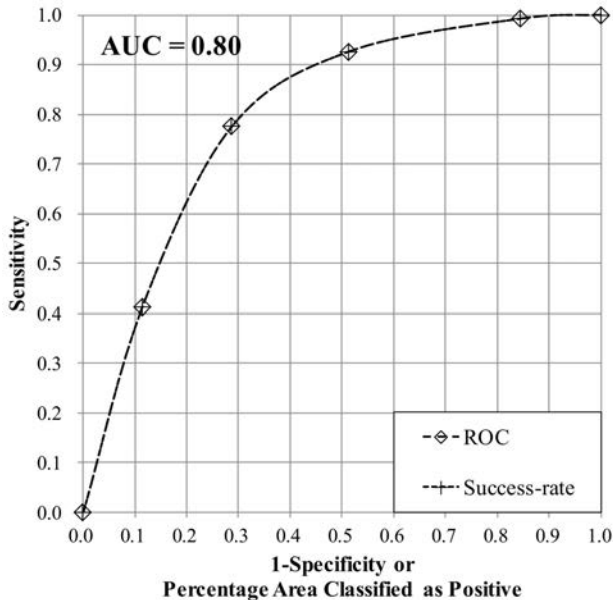
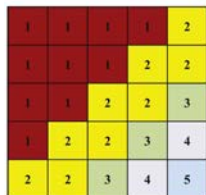


Figure 11

## Study Area A : High Hazard Area

### Susceptibility Map



### Number of pixels with landslide observed

|     |     |     |     |     |
|-----|-----|-----|-----|-----|
| 300 | 300 | 300 | 300 | 150 |
| 300 | 300 | 300 | 150 | 150 |
| 300 | 300 | 150 | 150 | 75  |
| 300 | 150 | 150 | 75  | 30  |
| 150 | 150 | 75  | 30  | 10  |

## Study Area B : Low Hazard Area

### Susceptibility Map



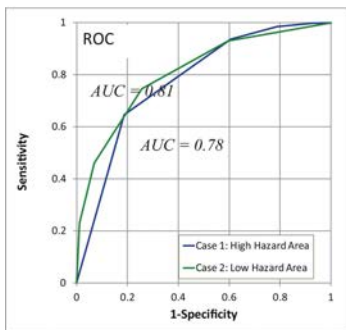
### Number of pixels with landslide observed

|     |     |    |    |    |
|-----|-----|----|----|----|
| 300 | 150 | 75 | 30 | 10 |
| 150 | 75  | 75 | 30 | 10 |
| 75  | 75  | 30 | 30 | 10 |
| 30  | 30  | 30 | 30 | 10 |
| 10  | 10  | 10 | 10 | 10 |

### Notes:

1. Each cell is assumed to represent 20 pixels by 20 pixels.
2. "1" denotes susceptibility class I (the most susceptible), while "5" denotes susceptibility class V (the least susceptible).

## ROC Curves



## Success-rate Curves

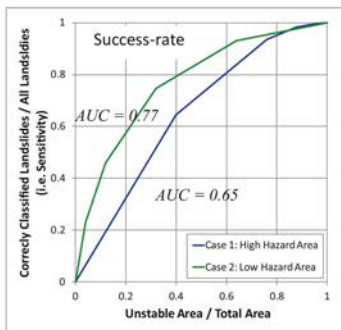


Figure 12